crystals

MDPI

Article

New Prediction Model for the Ultimate Axial Capacity of Concrete-Filled Steel Tubes: An Evolutionary Approach

Muhammad Faisal Javed [1,*], Furqan Farooq [1,*], Shazim Ali Memon [2,*], Arslan Akbar [3,*], Mohsin Ali Khan [4], Fahid Aslam [5], Rayed Alyousef [5], Hisham Alabduljabbar [5] and Sardar Kashif Ur Rehman [1]

1 Department of Civil Engineering, COMSATS University Islamabad, Abbottabad Campus, Abbottabad 22060, Pakistan; skashif@cuiatd.edu.pk
2 Department of Civil and Environmental Engineering, School of Engineering and Digital Sciences, Nazarbayev University, Nur-Sultan 010000, Kazakhstan
3 Department of Architecture and Civil Engineering, City University of Hong Kong, Kowloon 999077, Hong Kong
4 Department of Structural Engineering, Military College of Engineering (MCE), National University of Science and Technology (NUST), Islamabad 44000, Pakistan; moak.pg18mce@student.nust.edu.pk
5 Department of Civil Engineering, College of Engineering in Al-Kharj, Prince Sattam Bin Abdulaziz University, Al-Kharj 11942, Saudi Arabia; f.aslam@psau.edu.sa (F.A.); r.alyousef@psau.edu.sa (R.A.); h.alabduljabbar@psau.edu.sa (H.A.)
* Correspondence: arbabfaisal@cuiatd.edu.pk (M.F.J.); furqan@cuiatd.edu.pk (F.F.); shazim.memon@nu.edu.kz (S.A.M.); aakbar4-c@my.cityu.edu.hk (A.A.)

Received: 11 July 2020; Accepted: 20 August 2020; Published: 22 August 2020

Abstract: The complication linked with the prediction of the ultimate capacity of concrete-filled steel tubes (CFST) short circular columns reveals a need for conducting an in-depth structural behavioral analyses of this member subjected to axial-load only. The distinguishing feature of gene expression programming (GEP) has been utilized for establishing a prediction model for the axial behavior of long CFST. The proposed equation correlates the ultimate axial capacity of long circular CFST with depth, thickness, yield strength of steel, the compressive strength of concrete and the length of the CFST, without need for conducting any expensive and laborious experiments. A comprehensive CFST short circular column under an axial load was obtained from extensive literature to build the proposed models, and subsequently implemented for verification purposes. This model consists of extensive database literature and is comprised of 227 data samples. External validations were carried out using several statistical criteria recommended by researchers. The developed GEP model demonstrated superior performance to the available design methods for AS5100.6, EC4, AISC, BS, DBJ and AIJ design codes. The proposed design equations can be reliably used for pre-design purposes—or may be used as a fast check for deterministic solutions.

Keywords: concrete-filled steel tube (CFST); axial capacity; genetic engineering programming (GEP); Euler's buckling load; GEP-based model

1. Introduction

A concrete-filled steel tube (CFST), consists of a steel tube full of concrete. Over the last decade, their use in the building-construction industry as a column and has increased exponentially [1,2]. They have been used in various modern construction projects [3–6]. The CFST structure provides adamant structural advantages that include desirable ductility with high energy-absorption capacities, high strength and fire resistance [7–9]. During concrete construction, the use of shuttering is also not necessary for that reason, the concrete construction costs and the time is lowered. These advantages have been commonly exploited and contributed to the widespread use of CFST members in civil engineering structures [1]. The behavior of CFST members has been broadly examined in the last three decades. This study focuses on the CFST columns with a circular steel tube, as it offers more efficient stiffness and post-yield strength than those with a rectangular or square cross-section [10–12]. Many experimental studies are available on CFST circular columns, with a prime focus on strength of concrete [13–15], the diameter-to-thickness ratio of the tube [16–20] or bond action among steel tube and concrete [21–24].

In the last two decades, a variety of numerical and analytical studies on the behavior of CFST square columns under axial compression have been performed [13,14,16–20]. Nonetheless, the influence of confinement on the enhancement of concrete infilled strength has been held in different opinions. The effects of other variables—for example, the impact of dimension on the concrete strength—likewise varies among numerous researchers [25–27]. The empirical formulas developed for the post-buckling of the steel tube differ from study to study. [15]. Model expression of square CFST columns for the axial load capacity is available in ACI 318 (ACI 2014), Eurocode 4 (CEN 2004) and AISC 360 (AISC 2016). However, none of these equations agree with one another. Such models were derived from the pre-assumed stress–strain relationship of the steel tube or infilled concrete; thus, the validity of these models is doubtful. Moreover, experimental tests require much money, expensive testing equipment and human effort. The accuracy of experimental tests also depends on many factors including the type of equipment, skilled labor, proper casting of test specimens and proper instrumentation. In contrast, numeric studies require experimental tests for the validation. Moreover, numeric modeling demands high-performance workstations and high computational skills. Hence, an accurate empirical equation is required that is easy to use in most conditions and includes all important factors.

Researchers have suggested different methods and techniques for the prediction of the ultimate load-bearing capacity of long circular CFST columns [28,29]. For instance, least median, linear and nonlinear regression techniques are used by various researcher in different domains of civil engineering and have found profound effects [30–32]. This regression-based equation helps us in the prediction of structural domains—and even gives an adamant relation to target-based values. However, regression models are based on some assumptions, making them unrealistic in terms of prediction aspects [33,34]. To address this issue, deep learning in the field of machine-learning-based model algorithms have been developed that have had robust effects for model prediction [35]. In fact, this deep-learning models has been used by various researcher and proved its supremacy over traditional method [12,29]. Artificial neural network (ANN), gene expression programming with supervised learning algorithms are some method which helps in prediction of mechanical properties in the civil engineering domain [36,37]. Nguyen et al. used feed forward neural network (FNN) to predict the compressive strength of rectangular concrete steel filled tubes [38]. The author used invasion weed optimization (IWO) for tuning of parameters, and hence made a hybrid FNN–IWO model. This yielded strong correlation of 0.979 [38]. Hai et al. predict the strength of CFST by using surrogate models. The author used neuro-fuzzy inference system (ANFIS) with meta-based optimization methods to make hybrid algorithm [39]. Particle swarm optimization (PSO), genetic algorithm (GA) and biogeography-based optimization (BBO) are some techniques in prediction of CFST. The result reveals that use of PSO with ANFIS yield strong correlation of about 0.942 with less error [39]. Quang et al. used hybrid algorithm to predict the bearing capacity of rectangular concrete steel tube column [40]. One step secant (OSS) algorithm with FNN algorithm to make hybrid algorithm was developed. The result reveals a good strong model with minimum error between actual and predicted targets. Nguyen et al. used hybrid algorithm namely as GAP-BART which is based on Bayesian additive regression tree (BART) to predict the strength of CFST [41]. Genetic algorithm (GA), particle swarm optimization (PSO) was used in making hybrid approach. The author reveals that particle swarm optimization give adamant model performance with less error. These algorithms train the data to solve the desire problem and then test was conducted on testing set to give results. However, there exist some flaws in ANN modeling as it acts as a black box and does not give adamant relation to model in term of the equation. This reduces its chance of modeling perspective. Also, ANN parameters are based on several hit and trail cycles which in turn requires more time in prediction. In contrary, use of gene expression in supervised mechanism produces and gives a well-defined prediction model [42–44]. Ipek et al. predicted the axial capacity of concrete-filled double-skin steel column section by using gene expression [45]. The author achieved a strong correlation with actual and predicted one with minimum errors. The Gene expression model take the best input and optimize it and predict the outcome by minimizing its error and thus provide best prediction with adamant fitness. Numerous scholars' study and used GP in generating an accurate model for complex engineering domains. Different modifications were proposed to enhance the performance of GP. Genetic engineering programming (GEP) is the most advanced one. Yet, the use of GEP to address complex structural engineering problems has been limited [22]. Esra et al. estimated the axial carry capacity of concrete-filled tube by using GEP algorithm [46]. It is worth mentioning here, that the developed equation is two lengthy and cannot be used for practical implementation [47,48].

Experimental works is time consuming and thus required lot of resources to give a good justified strength. This tradition approach and misplacement of quantities during casting produces malignant effect to strength. Hence, use of supervised algorithms increases the efficiency of prediction by not only just taking data point, but can also help us in generating a hand-based equation. This equation can be then used to predict the overall efficiency of desired model. Moreover, supervised machine learning approaches just predict the strength by giving us the strong correlation but cannot give a relation-based equation. Hence, gene expression programming algorithm was used which can give a strong-based equation with stronger correlation with target and predicted values.

In this research, the GEP approach is exercised to evaluate the axial performance of CFST members. The developed model correlates the axial strength to a few affecting parameters. To effectively design the CFST members with lesser costs, it is essential to establish some models correlating the basic parameters with an axial ultimate capacity of CFST members. Special attention has been given in making a simplified equation that can predicts the strength of CFST even by hand calculation. The model proposed is built based on a huge number of published axial tests on CFST members. The results produced by the model developed are further than judged with those achieved through various codes of practice as several authors show their concerns about the existing design codes [23].

2. Comparison of Genetic Programming vs. Genetic Engineering Programming

Ferreira [24] proposed supervised learning machine algorithm ahead from GP which is based on the genetic human evolutionary algorithm. This modified form is also termed as gene expression programming (GEP). GEP develops computer supervised programs that are encrypted in fixed-length chromosomes whereas GP grows a solitary tree expression [49–51]. Gene expression programming (GEP) is like genetic algorithms (GA) and is an alternative form of traditional genetic programming (GP). It was proposed by Ferreira [24] and is used to predict the relationship between input and output data. In GEP the chromosome consist of linear, symbolic strings of genes and each gene in it is a code for object selection while expression tree (ET) is also used for the similar purpose. The parameters that are used by GEP are similar to the ones that were used in GP [52–54]. In these algorithms the computer programs consist of the characters of defined length comparing with the expression trees of length which varies in genetic programming. In computer programs each expression hide as cramped twine of rooted capacity and intentionally declared as the function in which entities are not affected by the change in their values. These types of programs are called complex tree structure or expression trees (ETs) [55–57]. GEP uses genotype and phenotype algorithms in which genotype is detached from phenotype and this programming results as an evolutionary advantage [24]. In GEP size of genome is defined clearly by the problems and is determined by hit and trial rule. For this purpose, a method that utilizes the capability of a system to choose a best possible mode of operation is adaptive control that is employed [58–60]. This approach uses the parameters that are same as of GP. Since all adaptation take place in simple linear structure because in overall structure mutation and structure replication is not required. Moreover, each chromosome comprises of genes which have two well-defined adjacent regions which is called head and the terminal symbols (nodes of leaf) called tail. In head the symbol are used to code internal on ET and in tail it is encoded in expression tree (ET) [61–63].

Figure 1 displays the GEP algorithm schematic layout. The procedure is started with the random formation of fixed dimension chromosome for each singular. Second, the genes are fetching as ETs and tested for their best fitness. Afterwards, the reproduction is applied to the individuals evaluated by the fitness function. The complete hierarchy is repetitive with newly produced gene until the obstinate solution is attained. In short, genetic procedures for example X-over, mutation and reproduction are used for the transformation in population.

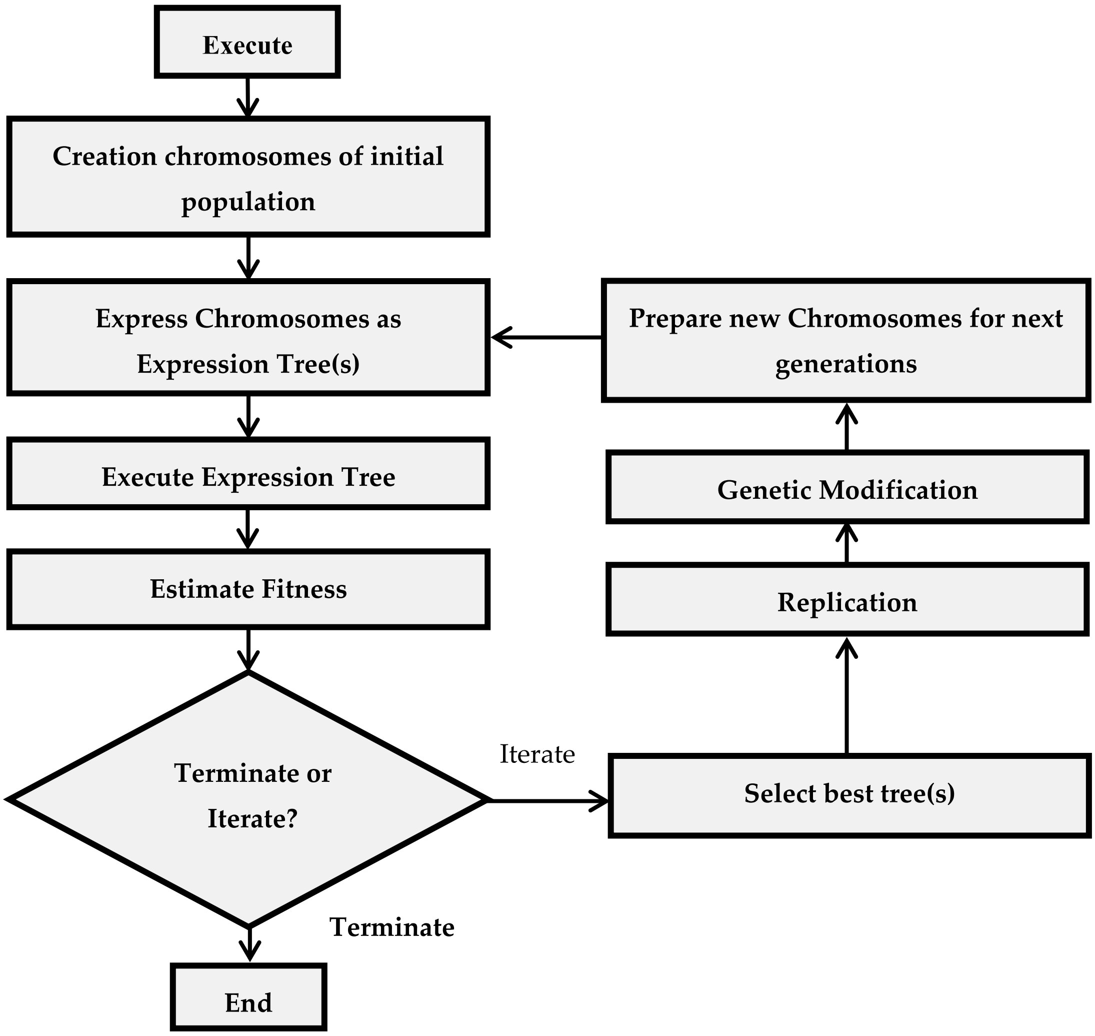

Figure 1. Simple illustration of the of the gene expression programming (GEP) algorithm [22].

3. Experimental Database

The model is built with the aid of 227 test results collected from more than 40 literature studies is attached in Appendix A. Only those results were included in the database in which no reinforcement in the infilled concrete is used. Frequency histograms are used for the visualization of the data distribution as shown in Figure 2. These distributions show the maximum parametric influence in total data points taken from literature. The maximum thickness of outer steel tube in CFST lies in the range of 3–5 mm. similarly, the maximum values of diameter, compressive strength, L/D lies in the range of 73–146 mm, 30–50 MPa and 7 to 20, respectively. This shows us the optimum variables values which when take in experimental work produce utmost effect with strength

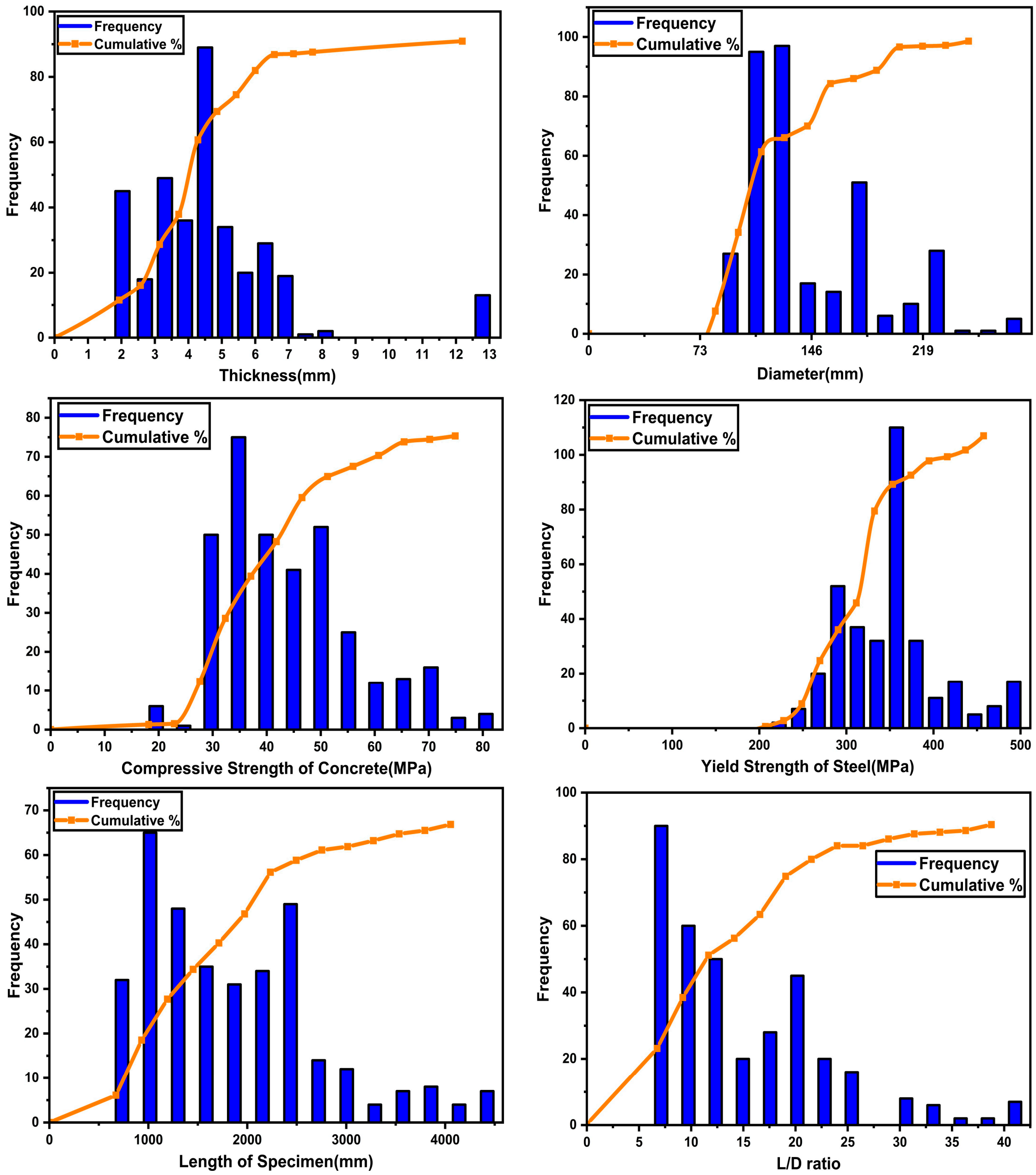

Figure 2. Histogram of the variables exercised in the establishment of the model.

The statistical parameters for the development of model including testing, training and validation set are shown in Table 1. Moreover, Figure 3 represents the relationship of individual variables with each other.

One major drawback comes in the supervised machine learning algorithms is the over fitting of data [64,65]. Abundant explanations have been recommended in the literature to evade this problem. Fulcher suggested to train and validate the data on different set of data [66]. In this study, this procedure is used by arbitrarily separating the obtainable data into three sets, namely as a validation set, learning set and testing set. First, the model is established created on the learning set or train set which is then validated by dividing set of data and finally test was conducted to evaluate the performance of model on test set [67]. The validated model is test on the data which is not used on train data.

Table 1. Descriptive variables statistics.

Parameters	Diameter	Thickness	Yield Stress	Compressive Strength	Length	Length/Diameter	Test
Training set data							
Mean	137.9	4.6	344.9	43.9	36.4	1651.8	13.0
Standard error	4.8	0.2	5.4	1.5	1.4	81.1	0.7
Median	114.3	4.1	338.9	40.5	33.4	1420.0	10.3
Mode	108.0	5.0	348.0	35.7	29.0	1040.0	20.0
Standard deviation	54.4	2.5	61.2	17.3	15.9	917.2	7.9
Sample variance	2956.3	6.2	3744.4	298.6	254.3	841,300.1	62.6
Kurtosis	4.6	3.8	0.2	3.4	4.3	2.6	3.9
Skewness	1.9	1.8	0.8	1.6	1.8	1.5	1.7
Range	279.6	11.4	271.8	91.6	86.0	4892.0	45.5
Minimum	76.0	1.4	233.2	14.4	10.0	508.0	4.5
Maximum	355.6	12.8	505.0	106.0	96.0	5400.0	50.0
Sum	17,646.2	592.2	44,143.2	5615.7	4656.1	211,432.9	1663.8
Count	128.0	128.0	128.0	128.0	128.0	128.0	128.0
Testing set data							
Mean	127.8	4.3	340.4	39.6	32.5	1806.0	15.0
Standard error	5.2	0.3	7.8	1.9	1.7	152.4	1.4
Median	114.0	4.0	340.0	35.7	29.0	1648.2	11.5
Mode	108.0	4.0	338.9	35.7	29.0	2700.0	6.0
Standard deviation	37.0	2.2	55.0	13.5	12.1	1077.3	9.9
Sample variance	1367.0	4.7	3021.6	182.2	147.1	1,160,607.4	97.2
Kurtosis	1.0	7.7	1.3	1.0	1.2	−0.2	0.4
Skewness	1.4	2.3	0.7	1.1	1.2	0.8	1.1
Range	136.5	11.3	267.8	62.8	57.2	3812.0	35.5
Minimum	82.6	1.4	237.2	14.4	10.0	508.0	4.5
Maximum	219.0	12.7	505.0	77.2	67.2	4320.0	40.0
Sum	6388.6	214.0	17,017.5	1982.3	1626.9	90,302.2	751.0
Count	50.0	50.0	50.0	50.0	50.0	50.0	50.0
Validation set data							
Mean	137.3	4.5	347.2	42.2	34.8	1755.6	13.8
Standard error	5.7	0.3	10.2	1.7	1.5	127.2	1.2
Median	114.3	4.1	338.9	40.2	33.0	1572.0	10.9
Mode	108.0	4.0	486.0	35.7	29.0	1640.0	6.0
Standard deviation	43.9	2.3	79.1	13.3	11.9	985.3	9.0
Sample variance	1927.1	5.1	6256.5	175.8	141.8	970,885.0	81.2
Kurtosis	0.4	4.5	1.0	0.5	0.9	2.3	3.8
Skewness	1.1	1.8	1.0	1.0	1.1	1.4	1.7
Range	190.9	11.4	404.5	57.5	52.8	4892.0	45.2
Minimum	76.5	1.4	200.2	25.5	20.2	508.0	4.8
Maximum	267.4	12.8	604.7	83.0	73.0	5400.0	50.0
Sum	8236.8	271.1	20,831.6	2534.8	2089.2	105,337.0	830.1
Count	60	60	60	60	60	60	60

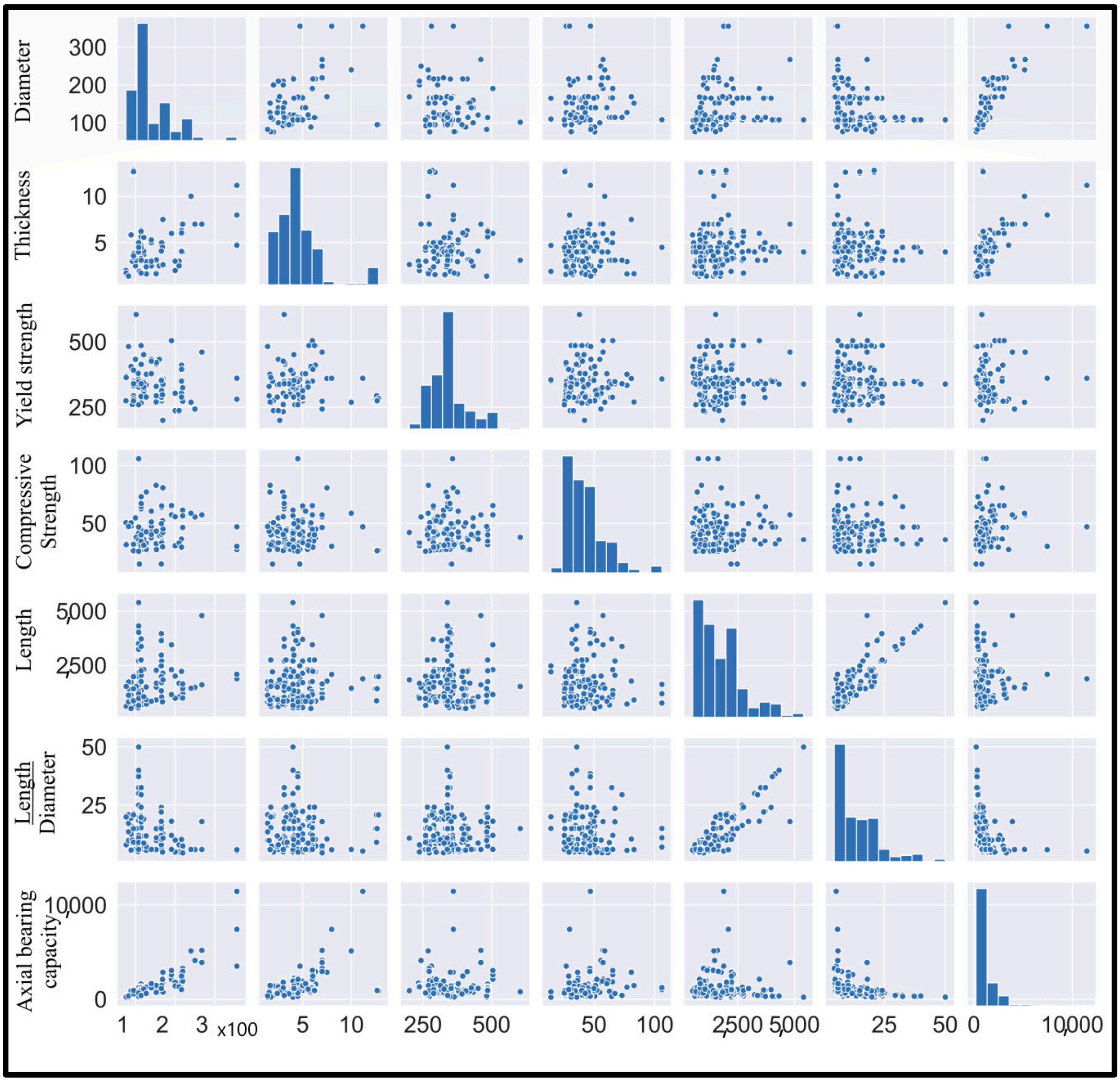

Figure 3. Relationship among individual variables.

Various parameters in designing long circular CFST members may be interdependent. Interdependency is needed to be check as it leads to difficulty in the interpretation of the model. In addition, the interdependency causes numerous problems during investigation as it upsurges the strength of relations between different parameters. This kind of problematic is often mentioned to as a "multicollinearity problem" [68]. Therefore, the association coefficients are calculated for all the possible mixtures among the parameters and are presented in Table 2. It can be detected that all the relation coefficients (both negative positive and) are not extraordinary, presentation no danger of "multicollinearity problem".

Table 2. Correlation coefficients for different variables.

Variable	Diameter	Thickness	Steel Yield Strength	Compressive Strength	Length	Length/Diameter
Diameter	1	0.367	−0.197	0.123	0.246	−0.293
Thickness	0.367	1	0.031	−0.041	0.091	−0.102
Steel yield strength	−0.197	0.031	1	0.088	−0.028	0.075
Compressive strength	0.123	−0.041	0.088	1	−0.016	−0.102
Length	0.246	0.091	−0.028	−0.016	1	0.813
Length/diameter	−0.293	−0.102	0.075	−0.102	0.813	1

4. Development of Model

The study aims in establishing a novel-based prediction equation for the axial compressive strength of CFST members using the GEP approach. The main variables frequently used in the earlier codes and analytical models were used as input variables. These parameters were evaluated based on the literature [15,21,69]. Therefore, the formulation of the axial ultimate strength of CFST member was assumed as follows:

$$N = f\left(D, t, f_y, f_c, L, \frac{L}{D}\right) \quad (1)$$

In the above equation, N is the ultimate axial capacities of the long circular CFST column. f_y, t, D *and* L are the yield strength, thickness, outer diameter and outer steel tube length, respectively. Whereas f_c is the 28-day compressive strength of concrete cylinder. The key input parameters used in the GEP algorithm are shown in Table 3. These variables have influence on model and thus importance should be given while selecting the governing one. Moreover, six basic mathematic operators (+, −, ÷, ×, square, cubic root) were used in predication of model.

Table 3. GEP parameters settings.

Parameter		Settings
General		
	Chromosomes	30
	Genes	3
	Head size	8
	Gene size	26
	Linking function	Addition
	Function set	$+, -, \times, \div, \surd, \sqrt[3]{}$
Genetic operators		
	Mutation rate	0.0138
	Inversion rate	0.00546
	IS Transposition rate	0.00546
	RIS transposition rate	0.00546
	One-point recombination rate	0.00277
	Two-point recombination rate	0.00277
	Gene recombination rate	0.00755
	Gene transposition rate	0.00277
Numerical constants		
	Constants per gene	10
	Data type	Floating Point
	Lower bound	−10
	Upper bound	10

The model prediction and time required to model is completely dependent on the difficulty of the problems, the population size and the variables. The model gets stopped after best fitness. In addition, gene size and chromosomes of the model have influence on the prediction of properties. Each gene size consists of a unique expression tree. The number of chromosomes in the genes and head size describes the difficulty level of GEP-based model. The overall fitness of the new programs is calculated via the mean absolute error (MAE) function. The parameters values included are calculated using trial and error. GeneXproTools 5.0 by Gepsoft Lda- Portugal was used to implement the GEP algorithm [70].

To achieve a consistent distribution of data, numerous arrangements of testing and training sets were established. The distribution of data in term of learning set, validation set and the model which predicts the response was used in GEP model to select the best response, namely as testing set. An objective function presented by Babanajad, Gandomi [71] is used to measure the fitness of learning and validation set. The finest GEP model was obtained by reducing the objective function (Equation (2)).

$$f_{min} = \left(\frac{n_L - n_V}{n_L + \ n_V}\right)\left(\frac{m_L + rm_L}{R_L^2}\right) + \frac{2n_V}{n_L + n_V}\left(\frac{m_V + rm_V}{R_V^2}\right) \tag{2}$$

In the above equation, n_V *and* n_L are the test numbers in validation sets and learning sets, respectively. R_L^2, m_L *and* rm_L are the determination coefficient, mean absolute error and root mean square error of learning set, respectively. R_V^2, m_V, *and* rm_V are the determination coefficient, mean absolute error and root mean square error of validation set, respectively. These all are calculated using the following equations. The mathematical forms of mean square error (MAE), root mean square error (RMSE) and determination coefficient are represented in Equations (3) and (4).

$$MAE = \frac{1}{n}\sum_{i=1}^{n}\left|x_i - y_i\right| \tag{3}$$

$$RMSE = \sqrt{\frac{1}{n}\sum_{i=1}^{n}(x_i - y_i)^2} \tag{4}$$

$$R = \frac{\sum_{i=1}^{n}(x_i - \overline{x}_i)\left(y_i - \overline{y}_i\right)}{\sqrt{\frac{1}{n}\sum_{i=1}^{n}(x_i - \overline{x}_i)^2\sum_{i=1}^{n}\left(y_i - \overline{y}_i\right)^2}} \tag{5}$$

In the above equations, x_i and y_i are the actual output and calculated output for the ith output, respectively. It is worth noting that the objective function presented in Equation (2) considers m, rm and R together, which results in a more accurate model. Furthermore, the given objective function takes into consideration the effect of distinct data sets, i.e., learning and validation sets. Lower values of m and rm indicates higher accuracy of the model.

5. Results and Discussion

The equation obtained for the ultimate axial capacity of circular CFST members is specified in Equation (6). The objective function (f_{min}) value obtained for Equation (2) is 182.52. Equation (6) is obtained from the expression tree which is shown in Figure 3. In Figure 4, the c1–c9 represents different constant values tried by the GEP, d0–d6 are different variables explained in Equation (1), while the 3Rt represents the cubic root of the value. It can be seen that the capacity of a concrete-filled steel tube is dependent on the input variables, namely as diameter, thickness, length to diameter ratio, yield strength, compressive strength as shown in Equation (6). Moreover, every parameter has a key influence on capacity thus increasing one or decreasing another will sufficiently have a benignant and malignant effect on its strength.

$$N_{GEP}(kN) = D(3t - 1) - t^2 - 137.67t - (4t + 1)\frac{L}{D} + \frac{f_y}{t} + 6.72f_c' + \left(f_y - L\right)^{\frac{1}{3}} - 46.61 \tag{6}$$

where N_{GEP} is the ultimate axial moment capacity of the column calculated from Equation (6) and f_c' is the compressive strength of infilled concrete. D, t, Land f_y are the diameter, thickness, length and yield strength of the steel tube, respectively.

The relationship between predicted values and experimental values is shown in Figure 5. The important statistical values of the proposed equation for learning, validation and testing sets are given in Table 4. It can be seen that the R^2 value was increased from 0.97 to 0.99 while MAE and RMSE decreases 134 to 124 and 210 to 173, respectively. Moreover, that the error value for testing is lesser as compared with other training and validation set. This illustrates that the present GEP model can accurately predict the axial capacity of CFST members and can be used for the generalization purpose [72].

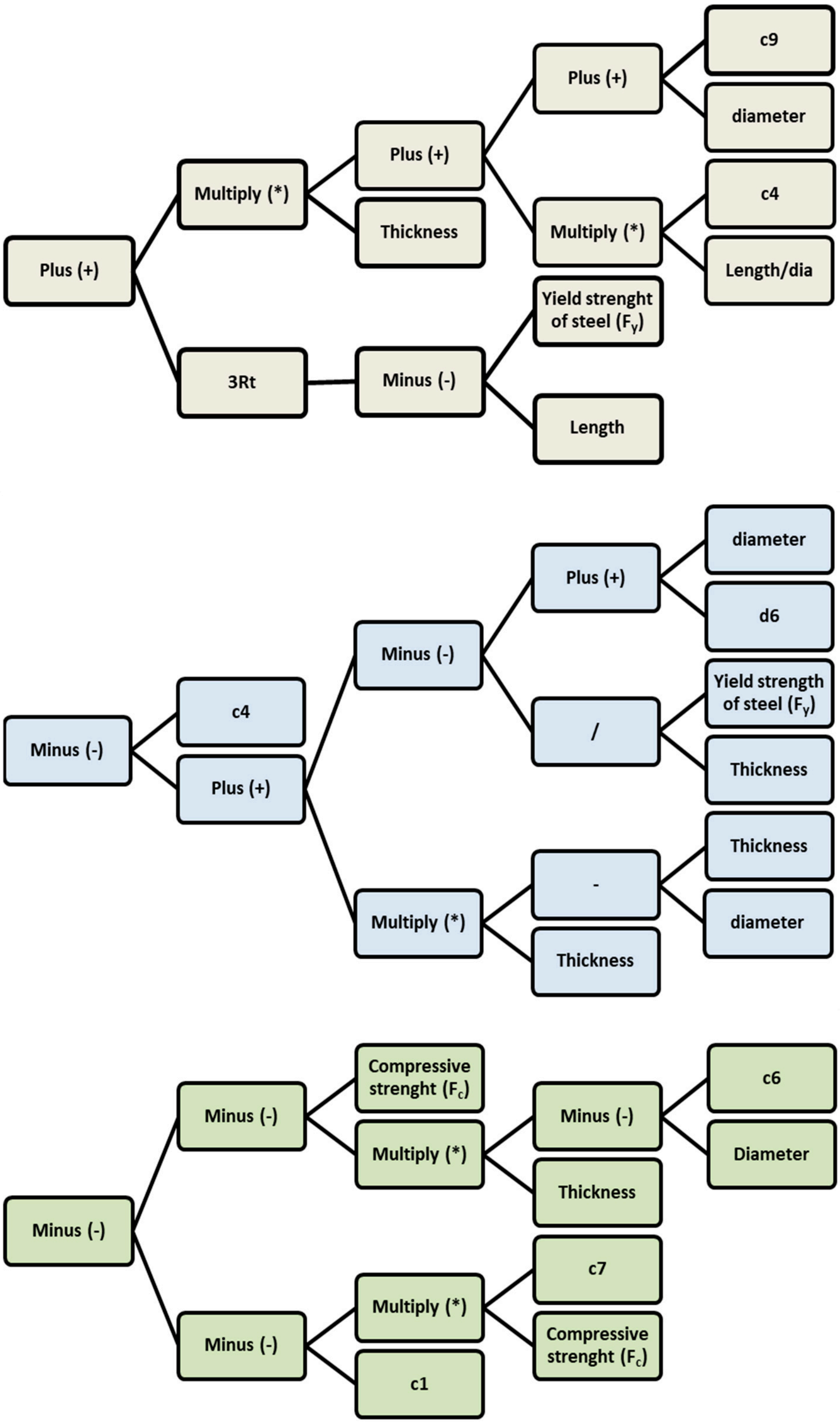

Figure 4. Expression tree for the GEP model.

Table 4. GEP model execution results.

Model	Experimental Axial Capacity vs. Predicted Axial Capacity		
	R^2	MAE	RMSE
Learning	0.97	134.8	210.3
Validation	0.98	153.9	226.1
Testing	0.99	124.3	173.7

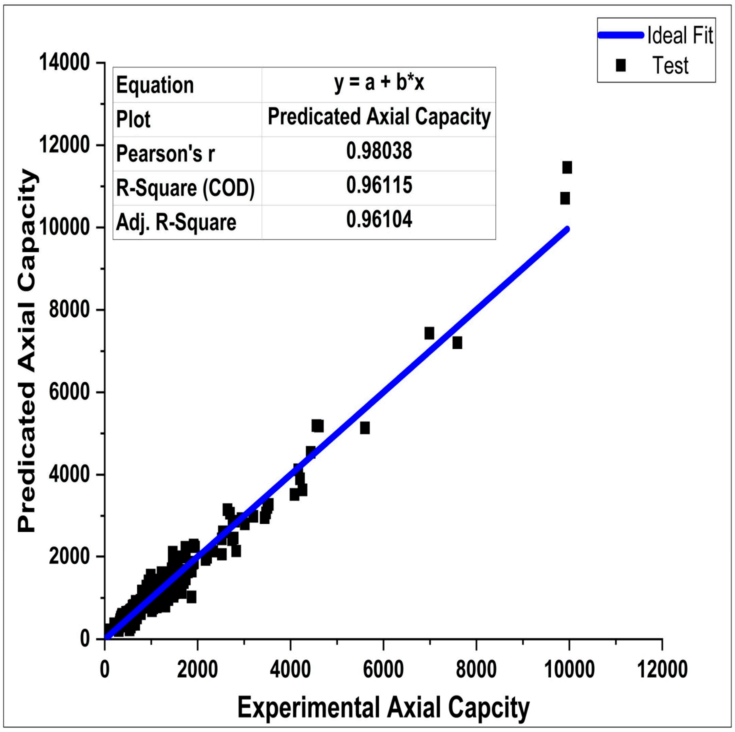

Figure 5. Predicted axial capacity vs. experimental results using the GEP model.

Model Performance, Validity and Comparative Study

The existing formulae provided by six different design codes (AS5100.6 (2004), EC4 (2004), AISC, BS, DBJ, AIJ) are utilized for the comparison of the suggested model. The process for the calculation of the axial load capacity of circular CFST columns is described in Table 5. The Australian standard (AS5100.6) counteract for the interaction effect of and steel tube concrete core. It also contains the effectiveness of concrete confinement. The relation presented by British standard (BS5400) contains an allocation for the eccentricity of the minor axis that does not surpass 0.03 times the composite column's least lateral dimension. It is improper as the engineer's preference may increase it. The equation of the American Institute of Steel Construction (AISC 2005) accounts for the effect of the restraining hoop that results from transverse confinement. This phenomenon increases the usable concrete stress. The relation provided by the Architectural Institute of Japan (AIJ 2001) involves a confinement factor that accounts for the reduction in the steel tube effective yield stress, caused by the hoop stresses. In the Eurocode 4 (EC4 2004), the equation accounts for the confinement effect in addition to the effect of steel tube and concrete core interaction. The concrete strength is increased by the triaxial state of stress conditions and the hoop stress that reduces the steel effective yield stress. The Chinese code (DBJ 1999) provides an equation ultimate axial moment capacity that cannot be used for ultra-high-strength concrete.

The comparison between the predicted values from the GEP model and different established codes is shown in Figure 6. In Figure 6, the model accuracy is highest for the value of 1. The frequency of 1 is highest for the GEP model while it is lowest for AS5100.6. In addition, it can be seen from the below Figures that the frequency of all the codes lies above 1. Thus, minimizing its practical implementation in calculation of strength. On the other side, GEP model show the distribution of its frequency in the range of 0 and 1. Thus, making it a safe approach in prediction. The statistical parameters for the comparison purpose are shown in Table 6. The R-value must approach to 1 for maximum accuracy. A value of R greater than 0.8 is deemed acceptable [73]. GEP model gives the best results than the available design codes. Furthermore, the MAE and RMSE are calculated for available design codes and the GEP model. Both MAE and RMSE should be minimum for higher accuracy. Based on MAE and RMSE, GEP gives the most accurate results followed by AIJ and BS, respectively.

Table 5. Details of the codes.

Equation No:	Code Specification	Ultimate Axial Moment Capacity (N_U)	Limitations
1	AS5100.6 (2004)	$N_u = \alpha_c\left[\eta_a A_s f_y + \left(1 + \frac{\eta_c t f_y}{d_o f'_c}\right)A_c f'_c\right]$ $\alpha_c = \xi\left(1 - \sqrt{1 - \left(\frac{90}{\xi\lambda}\right)^2}\right);\ \xi = \frac{\left(\frac{\lambda}{90}\right)^2 + 1 + \eta}{2\left(\frac{\lambda}{90}\right)^2}$ $\lambda = \lambda_n + \alpha_a\alpha_b\ ;\ \eta = 0.00326(\lambda_n - 13.5) \geq 0\ ;\ \lambda_n = 90\lambda_r$ $\lambda_r = \sqrt{\frac{N_s}{N_{cr}}}\ ;\ N_s = A_s f_y + A_c f'_c$ $N_{cr} = \frac{\pi^2 (EI)_{eff}}{l^2};\ (EI)_{eff} = E_s I_s + E_c I_c$ $\alpha_a = \frac{2100(\lambda_n - 13.5)}{\lambda_n^2 - 13.5\lambda_n + 2050};\ \alpha_b = Presented\ in\ code$ $\eta_2 = 0.25(3 + 2\lambda_r) \geq 0\ ;\ \eta_1 = 4.9 - 18.5\lambda_r + 17.5\lambda_r^2 \geq 0$	
2	AISC (2005)	$N_u = \phi_c N_n\ ;\ \phi_c = 0.75\ (LRFD)$ $If\ N_e \geq 0.44N_o\ ; N_n = N_o\left[0.658^{\left(\frac{N_o}{N_e}\right)}\right]$ $If\ N_e < 0.44N_o\ ;\ N_n = 0.877N_e$ $N_o = A_s f_y + 0.95A_c f'_c$ $N_e = \frac{\pi^2 (EI)_{eff1}}{(KL)^2}\ ;\ EI_{eff1} = E_s I_s + C_1 E_c I_c$ $C_1 = 0.1 + 2\left(\frac{A_s}{A_c + A_s}\right) \leq 0.3\ ;\ E_c = (f'_c)^{\frac{1}{2}}\ (MPa)$	$21\ MPa \leq f'_c \leq 70\ MPa$ $f_y \leq 525\ MPa$ $A_s \geq 0.01A_g$ $\frac{D}{t} \leq \sqrt{\frac{8E_s}{f_y}}$
3	BS5400	$\alpha_c = \frac{0.45 f_{cc} A_c}{N_u}\ ; 0.1 < \alpha_c < 0.8$ $N_u = 0.91 f'_y A_s + 0.45 f_{cc} A_c$ $f'_y = C_2 f_y\ ;\ f_{cc} = f_{cu} + C_1 \frac{t}{D} f_y$ $C_1\ and\ C_2 are\ constants\ depends\ on\ \frac{l_e}{D}$	$f_{cu} \geq 20\ MPa$ $f_y = Grade\ 43\ or\ 50$ $\frac{D}{t} \leq \sqrt{\frac{8E_s}{f_y}}$ $Nominal\ aggregate\ size \leq 20\ mm$
4	DBJ (1999)	$N_u = \gamma_m f_{scy} W_{scm}$ $f_{scy} = (1.18 + 0.85\xi) f_{ck}$ $W_{scm} = \frac{\pi}{32} D^3$ $\xi = \frac{A_s f_{yk}}{A_c f_{ck}}$ $\gamma_m = 1.04 + 0.48 \ln(\xi + 0.1)$	$100\ mm \leq D \leq 2000\ mm$ $200\ MPa \leq f_{scy} \leq 500\ MPa$ $20\ MPa \leq f_{ck} \leq 80\ MPa$

Table 5. *Cont.*

Equation No:	Code Specification	Ultimate Axial Moment Capacity (N_U)	Limitations
5	AIJ (2001)	$N_{u1} = 0.85A_c f_c' + (1+\eta)A_s f_y\ ;\left(\frac{l}{D} \leq 4\right)$ $N_{u2} = N_{u1} - 0.125\{N_{u1} - N_{u3}\}\left(\frac{l}{D} - 4\right);\left(4 < \frac{l}{D} \leq 12\right)$ $N_{u3} = A_c\sigma_{cr} + N_{crs}\ ;\left(\frac{l}{D} > 12\right)$ $\sigma_{cr} = \frac{1.7f_c'}{1+\sqrt{\lambda_1^4+1}}\ ;\ \lambda_1 \leq 1.0$ $\sigma_{cr} = 0.83\exp\{(0.568+0.00612f_c')(1-\lambda_1)\}0.85f_c'\ ;\ \lambda_1 > 1$ $\lambda_1 = \frac{\lambda}{\pi}\sqrt{0.93(0.85f_c')^{\frac{1}{4}} \times 10^{-3}}$ $N_{crs} = A_s f_y\ ;\ \lambda_1 \leq 0.3$ $N_{crs} = 1 - 0.545(\lambda_1 - 0.3)\ ;\ 0.3 \leq \lambda_1 < 1.3$ $N_{crs} = \frac{N_{Es}}{1.3}\ ;\ \lambda_1 \geq 1.3$ $\lambda_1 = \frac{\lambda}{\pi}\sqrt{\frac{f_y}{E_s}}$ $N_{Es} = \frac{\pi^2 E_s I_s}{l^2}$ $\lambda = slenderness\ ratio\ of\ concrete\ column$	$\frac{D}{t} \leq \frac{35250}{f_y}$
6	EC4 (2004)	$N_u = \eta_a A_s f_y + \left(1 + \eta_c \frac{t}{D}\frac{f_y}{f_c'}\right)A_c f_c'$ $\eta_a = 0.25\left(3+2\overline{\lambda}\right) \leq 1.0\ ;\ \eta_c = 4.9 - 18.5\overline{\lambda} + 17\overline{\lambda}^2 \geq 0$ $\overline{\lambda} = \frac{N_{plR}}{N_{cr}};\ N_{plR} = A_s f_y + A_c f_c'$ $N_{cr} = \frac{\pi^2(EI)_{eff2}}{l_2};\ (EI)_{eff2} = E_s I_s + K_c E_c I_c;\ K_c = 0.6$ $E_c = 22,000\left[\frac{(f_c'+8)}{10}\right]^{0.3}(MPa)$	$20\ MPa \leq f_c' \leq 60\ MPa$ $f_y \leq 460\ MPa$ $\frac{D}{t} \leq \frac{0.15E_s}{f_y}$

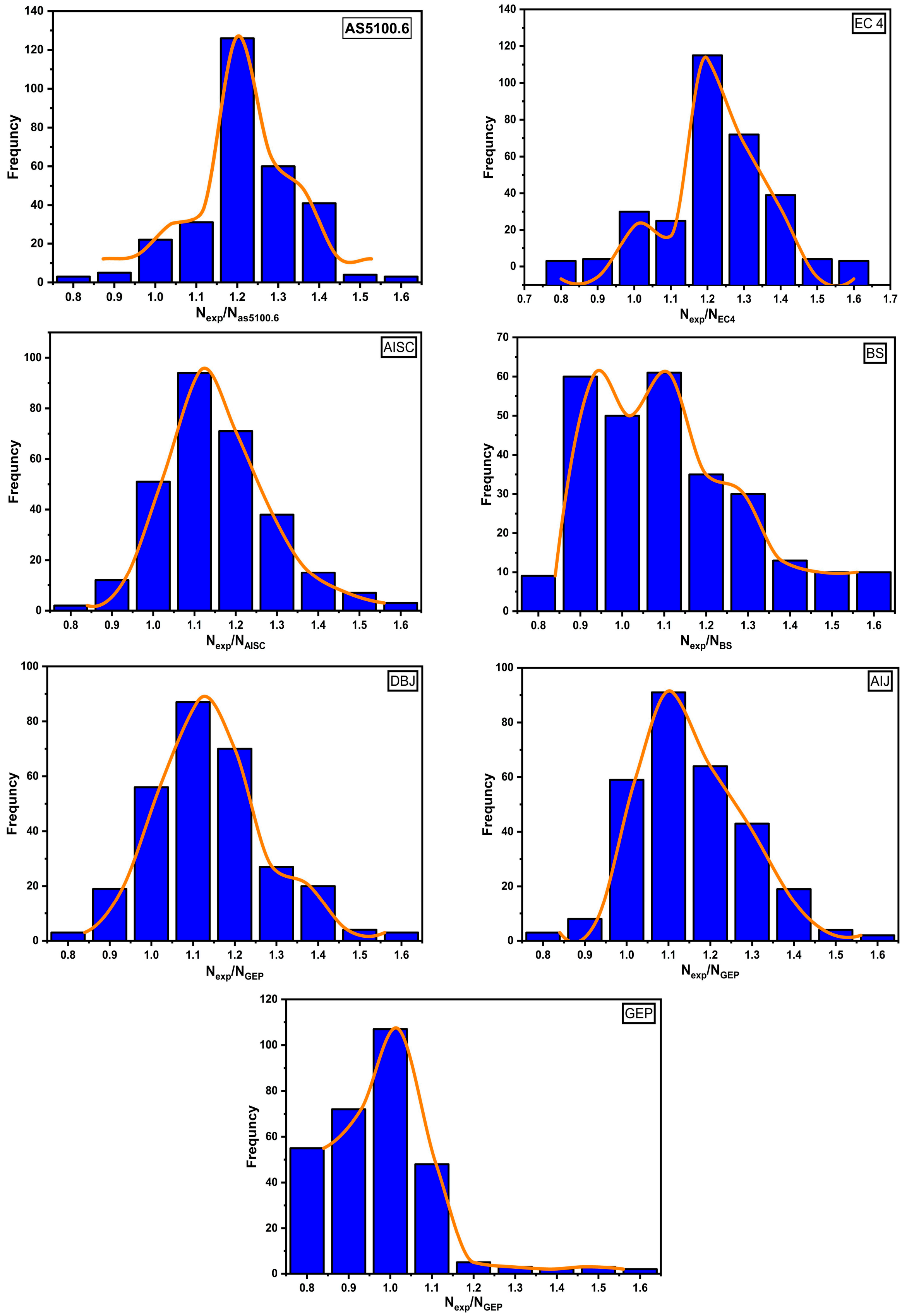

Figure 6. Evaluation of the concrete-filled steel tubes (CFST) columns experimental and predicted axial bearing capacity.

Table 6. Axial strength prediction models overall performance.

Statistical Parameters	GEP	AS5100.6	EC4	AISC	BS	DBJ	AIJ
Rsq	0.98	0.98	0.98	0.97	0.96	0.97	0.97
MAE	138.7	249.4	220.6	333.5	205.0	228.0	194.4
RMSE	258.0	484.7	452.9	701.4	352.9	512.0	408.4
Row (ρ)	0.1	0.2	0.1	0.2	0.3	0.2	0.2
Average	1.2	1.1	1.2	1.0	1.0	0.9	1.2
Maximum	1.2	1.6	1.7	2.0	1.7	1.5	1.2
Minimum	0.7	0.7	0.8	0.6	0.5	0.6	0.8
SD	0.1	0.1	0.1	0.1	0.3	0.2	0.1
COV	0.1	0.1	0.1	0.1	0.2	0.1	0.1

The model evaluation between errors and performance coefficient is measured by performance index (ρ) [74]. ρ is used successfully by numerous researchers and is calculated by using Equation (7):

$$\rho = \frac{Rr_m}{1+R} \tag{7}$$

where Rr_m is the relative r_m. Higher value of ρ shows bad achievement of the model and vice versa. From Table 6, it is determined that the GEP model outperforms the available design codes by huge margin.

The model accuracy can also be checked by several statistical measures. Frank and Todeschini [74] proposed that the accuracy of model is based on the number of testing set and the numbers of parameters used in modeling. He suggested and equation in which the ratio of both aforementioned should be greater than or equal to 5 as presented in Equation (8):

$$\frac{No.\,of\ experimental\ tests}{No.\,of\ variables\ used} \geq 05 \tag{8}$$

In this research, the ratio is 44. Furthermore, external verification is also suggested by researcher [75]. The test recommended that the slope of one of the regression lines moving through the origin should be approximately 1 [76]. In addition, test recommended by Roy [77] was also conducted for the given model. Table 7 outlines the acceptance benchmarks and the results of the built GEP model. The model developed based on GEP adamantly fulfils the criteria of all the above-mentioned tests. It is therefore inferred that the GEP model established is accurate and is not a simple correlation.

Table 7. GEP model statistical parameters for external validation.

Sr. No	Formula	Condition	GEP
1	Equation (5)	$R > 0.8$	0.973
2	$K = \frac{\sum_{i=1}^{n}(x_i \times y_i)}{x_i^2}$	$0.85 < K < 1.15$	0.983
3	$K' = \frac{\sum_{i=1}^{n}(x_i \times y_i)}{y_i^2}$	$0.85 < K' < 1.15$	1.003
4	$R_m = R^2 \times \left(1 - \sqrt{\lvert R^2 - R_0^2 \rvert}\right)$	$R_m > 0.5$	0.838
R_0^2 is squared correlation coefficient between predicted and experimental values			0.999

Simplicity is the utmost advantages in prediction of mechanical properties based on GEP algorithm. This adamant advantage helps in calculation of ultimate axial capacity by hand calculations using GEP-based formula. GEP model is completely independent and does not depend on the previous equations and design models. Moreover, increasing the training and validation set data enhance the overall accuracy of the model.

A comparison of GEP model with equations suggested by various authors was made on all data set [78–80]. It can be seen in Figure 7 that GEP model give an adamant R^2 accuracy of about

0.94 as compared to other models. This is due to simplified nature of GEP in prediction. Moreover, Glakoumelis et al. [80] predict the compressive nature of CFST by giving an empirical relation with a strong correlation value R^2 of about 0.895. Also, Goode et al. [79] and Lu et al. [78] give same empirical equation with some modification with R^2 value of 0.807 and 0.903, respectively as illustrated in Figure 7. This study show us that GEP-based empirical equations can be used in prediction of different variables.

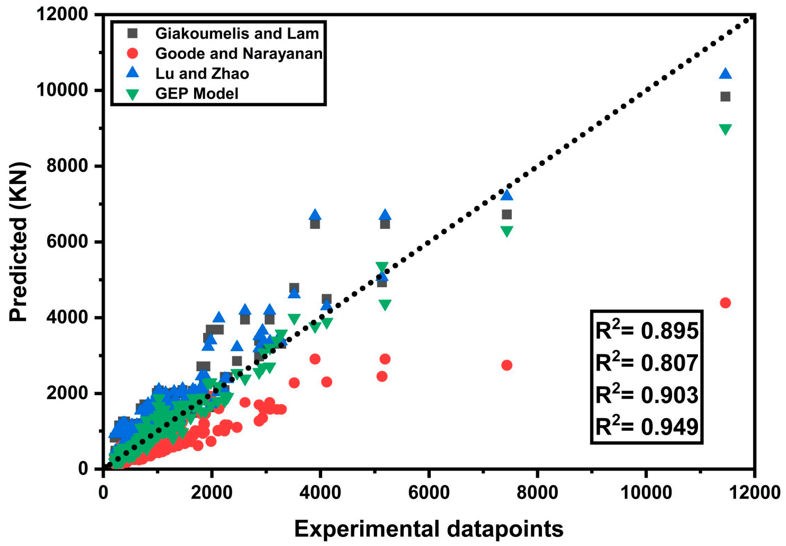

Figure 7. Comparison of GEP model with other published equations [78–80].

6. Conclusions

This study represents a novel and dominant method for the derivation of the expression to compute the ultimate axial capacity of CFST long circular columns by genetic engineering programming (GEP) for the first time. The resulting equation is empirical, and is formed by previous experimental data published in literatures. The suggested equation is simplest and CFST axial capacity can be determined by hand calculations. All the model outcomes show outstanding consent to the experimental results. Different statistical parameters such as RMSE, MAE and R^2 proved the accuracy and reliability of GEP-based derived equations. In addition, this supervised machine learning algorithm can be used in many other domains. As they help us in making the forecast prediction by training and testing of data. This artificial intelligence-based algorithm then helps scientific community by taking measures and overcome the issues associated in mechanical work or in experimental work. Though, the comparison between the MAE, RMSE and R^2 of GEP model, AS5100.6, EC4, AISC, BS, DBJ and AIJ shows that GEP model performs best for all sets (learning, training and validation) of data. Even though the GEP-based model can calculate short CFST shear strength, it is restricted to long circular columns. The findings from this new research will give civil engineers and structural designers some useful information and can be used as a modern and powerful method to help decision-making in concrete construction fields.

Author Contributions: Fahid Aslam (F.A.); visualization and Conceptualization, Muhammad Faisal Javed (M.F.J.); Conceptualization, Furqan Farooq (F.F.); software and Investigation, Arslan Akbar (A.A) and Mohsin Ali Khan (M.A.K.); writing—review and editing; Shazim Ali Memon (S.A.M.); writing—review & editing, Project administration, Funding acquisition", Rayed Alyousef (R.A.); review & editing; Hisham Alabduljabbar (H.A.); Review and Graphs; Sardar Kashif Ur Rehman (S.K.U.R.); review & editing. All authors have read and agreed to the published version of the manuscript.

Funding: This research was supported by Nazarbayev University Faculty development competitive research grants (090118FD5316) and deanship of scientific research at Prince Sattam Bin Abdulaziz University under the research project number 2020/01/16810.

Acknowledgments: The authors acknowledge the support of COMSATs University Islamabad, Abbottabad Campus and Engr. Kashif Nazir for providing fruitful environment in completing this research.

Conflicts of Interest: The authors declare no conflict of interest.

Nomenclature

CFST = Concrete-filled steel tube
ANN = Artificial neutron network
GP = Genetic programming
GEP = Genetic engineering programming
ETs = Expression trees
MAE = Mean absolute error
$RMSE$ = Root mean square error
N_u = Ultimate axial moment capacity
N_n = Nominal axial moment capacity
N_e = Euler's bucking load
N_o = Nominal axial compressive strength exclusive of length effects
A_s = Steel section areas
A_c = Concrete area
A_g = Total composite cross-section area
D = Diameter of concrete core
E_c = Concrete elastic modulus $= 0.043\omega_c^{1.5}\sqrt{f_c'}$ MPa
E_s = Steel elastic modulus $= 200,000$ MPa
f_c' = Concrete compressive strength
f_y = Steel section minimum yield strength
I_c = Concrete section moment of inertia
I_s = Steel section moment of inertia
K = Length effectiveness factor
L = Length of laterally braced member
$(\mathrm{EI})_{eff}$ = Composite section effective stiffness
N_e = Elastic bucking load
α_c = Concrete contribution factor
f_{cu} = 28-day characteristic strength of concrete cube
f_{cc} = Triaxially contained concrete improved characteristic strength
f_{scy} = Steel-tube nominal yield strength
f_{ck} = Concrete characteristic strength
f_y' = Reduced nominal yield strength of the steel casing
l_e = Effective length $= 0.7l$
l = Actual length
η_c = Concrete confinement coefficient
η_a = Steel tube confinement coefficient
$\overline{\lambda}$ = Relative slenderness
$(EI)_{eff2}$ = Effective flexural stiffness
K_c = Correction factor
η = Confinement factor $= 0.27$
ξ = Confinement factor
W_{scm} = Section modulus of composite cross section
γ_m = Flexural strength index
f_{min}= Objective function

Appendix A

Table A1. Data used to model concrete-filled steel tube.

S. No	Diameter	Thickness	Yield Strength	Compressive Strength	Length	Length/Diameter	Axial Capacity
1	120.9	3.73	312	30.22	2311	19.11	725
2	166	5	288.1	63.70	1040	6.27	1862
3	88.9	5.842	406	50.50	1117.6	12.57	715.56
4	114.3	3.1	348	62.78	670	5.86	898
5	95	3.68	392	31.44	860	9.05	686
6	166	5	288.1	36.55	1040	6.27	1495
7	168.2	4.52	302	52.80	813	4.83	2113
8	114.3	3.1	348	62.78	670	5.86	904
9	219	7	273	46.50	1200	5.48	3200
10	114	6.34	486	45.00	850	7.46	1608
11	100	2.5	433.2	54.78	600	6.00	750
12	108	4	338.88	35.71	5400	50.00	210.7
13	219	7	273	46.50	1420	6.48	3070
14	215.9	4.08	292	28.67	2220	10.28	1650
15	152.4	1.55	294	43.25	914	6.00	721.5
16	114	6	486	45.00	850	7.46	1334
17	114.3	3.1	340	73.10	3370	29.48	379
18	95	3.66	338	30.00	2032	21.39	463
19	216	4.04	293	36.89	2220	10.28	2289
20	114.3	3.19	414	35.44	838	7.33	734
21	95	12.4	277	26.22	1420	14.95	907
22	108	4	337.6	43.12	756	7.00	785
23	152.4	1.55	330	32.11	1499	9.84	734
24	166	5	288.1	65.17	1040	6.27	1852
25	166	5	289.1	34.68	2700	16.27	1117.2
26	110	1.9	350	14.44	2200	20.00	252
27	120.9	3.76	312	26.78	1049	8.68	721
28	216	4.11	291	36.89	2220	10.28	2239
29	108	4.5	348.1	46.87	4023	37.25	318
30	190.7	6	505	57.40	3450	18.09	2130
31	166	5	288.1	53.11	1040	6.27	1695
32	108	4	338.88	35.71	864	8.00	766.36
33	95	12.75	277	26.22	1420	14.95	938
34	114	5.94	486	45.00	1750	15.35	1138
35	216	4.11	304	29.11	2220	10.28	1834
36	152.4	3.17	415	26.56	2271	14.90	939
37	114	4.68	332	45.00	850	7.46	1049
38	108	4.5	259.7	25.48	1620	15.00	524
39	108	4	338.88	35.71	3240	30.00	478.24
40	110	1.9	350	14.44	2200	20.00	219
41	76.48	1.73	369	32.56	609.45	7.97	330.04
42	166	5	274.4	36.43	1100	6.63	1985
43	127.1	2.95	376	77.20	711	5.59	1305
44	114.3	3.1	348	62.67	1020	8.92	888
45	110	1.9	350	40.50	2200	20.00	437
46	355.6	11.18	361	47.00	1880	5.29	11,460
47	88.9	5.85	400	49.75	508	5.71	992
48	127.3	1.63	334	77.20	711	5.59	1285
49	210	3	233.2	33.52	1040	4.95	1705
50	114.3	3.1	340	64.56	3720	32.55	293
51	355.6	4.72	281	27.00	1880	5.29	3517
52	114	3.41	291	43.75	2750	24.12	569
53	95	3.66	332	31.44	860	9.05	656
54	95	12.7	277	26.22	860	9.05	1034
55	108	4.5	358	106.00	1188	11.00	1194
56	121	3.73	333	27.11	1050	8.68	746
57	219	7	273	46.50	990	4.52	3278
58	168.4	4.52	302	52.80	813	4.83	2233
59	160	2.5	433.2	39.40	960	6.00	1426
60	121	3.71	313	30.67	2310	19.09	695
61	88.9	5.842	406	50.50	1422.4	16.00	712
62	88.9	5.72	400	48.25	1422	16.00	712
63	165.2	4.1	353	49.88	3965	24.00	1019
64	168.1	4.52	298	52.30	813	4.84	2233
65	92	3	260.7	26.07	1380	15.00	409
66	114	5.94	486	31.11	1280	11.23	1285
67	114	6.11	486	40.00	2750	24.12	941
68	168.8	5	302.4	40.50	2135	12.65	1130
69	108	4.5	348.1	31.91	4158	38.50	342

Table A1. *Cont.*

S. No	Diameter	Thickness	Yield Strength	Compressive Strength	Length	Length/Diameter	Axial Capacity
70	82.55	1.397	482.3	47.29	1422.4	17.23	294.59
71	114	3.23	290	36.67	1751	15.36	706
72	121	5.41	348	27.11	1050	8.68	1018
73	165.2	4.17	358.7	49.82	1321.6	8.00	1445
74	95	3.86	332	31.44	1420	14.95	567
75	95	12.6	279	26.22	860	9.05	1018
76	166	5	289.1	34.68	2700	16.27	1271.06
77	114.3	3.1	348	65.56	1335	11.68	794
78	108	4.5	358	106.00	1620	15.00	1018
79	114.3	3.1	348	67.22	2040	17.85	688
80	250	7	243	55.58	1480	5.92	4116
81	76.5	1.74	364	49.88	610	7.97	423
82	95	3.91	392	31.44	1420	14.95	606
83	108	4.5	358	106.00	756	7.00	1286
84	165	4.7	355	33.40	2475	15.00	1058
85	114	1.72	266	43.75	2750	24.12	353
86	95	12.6	275	25.89	1981	20.85	903
87	200	3	303.5	55.80	2002	10.01	1882
88	169	7.5	360	80.80	1768	10.46	2870
89	152.4	3.17	415	26.56	2271	14.90	881
90	121	3.86	332	30.67	2310	19.09	755
91	165.2	4.17	358.7	49.82	1982.4	12.00	1305
92	95	12.5	279	26.22	1420	14.95	947
93	108	4.5	348.1	31.91	3510	32.50	400
94	88.9	5.82	400	48.75	1727	19.43	614
95	88.9	5.842	406	50.50	812.8	9.14	918.925
96	166	5	288.1	52.90	1040	6.27	1764
97	121	5.44	327	30.67	2310	19.09	865
98	169.3	2.62	338.1	41.38	1830	10.81	689
99	121.01	3.66	300	27.11	1050	8.68	695
100	108	4	338.88	35.71	2160	20.00	672.28
101	166	5	284.2	51.24	870	5.24	1862
102	108	5	379.8	40.91	548	5.07	1084
103	114	3.35	291	45.00	850	7.46	785
104	108	4	338.88	35.71	1620	15.00	646.8
105	76.5	1.73	364	32.11	610	7.97	330
106	355.6	7.98	361	29.78	2083	5.86	7433
107	114	1.79	266	45.00	850	7.46	515
108	267.4	7	461	57.40	4800	17.95	3900
109	95	12.6	294	26.22	1980	20.84	917
110	114.3	3.1	348	62.67	1020	8.92	849
111	108	4.5	358	106.00	1188	11.00	1232
112	76	2	275	50.60	1556	20.47	330
113	216	6.3	411	36.89	2220	10.28	2932
114	114	5.73	486	40.00	2750	24.12	824
115	110	1.9	350	33.40	2200	20.00	374
116	219	4	325	61.44	1000	4.57	1980
117	267.4	7	461	57.40	1600	5.98	5190
118	88.9	5.81	400	47.62	1118	12.58	716
119	121	3.76	313	30.67	1050	8.68	837
120	108	4	338.88	35.71	2160	20.00	676.2
121	127	2.413	336	32.56	914	7.20	658.3
122	120.83	4.09	451.3	36.18	1050.04	8.69	1091.91
123	200	3	303.5	55.80	2001	10.01	1806
124	108	4	338.88	35.71	1080	10.00	783.02
125	82.55	1.397	482.3	47.29	1727.2	20.92	224.725
126	121.01	3.71	300	27.11	2310	19.09	641
127	140	2.5	433.2	47.43	840	6.00	1124
128	152.4	1.57	330	26.67	1499	9.84	681
129	120.65	4.09	451.3	41.72	1050.04	8.70	1155.7
130	215.9	6.02	350	36.44	2220	10.28	2869
131	121	5.49	348	27.11	2310	19.09	816
132	200	2	237.2	30.28	980	4.90	1411
133	82.55	1.397	482.3	47.29	812.8	9.85	400.5
134	108	4	338.88	35.71	2700	25.00	648.76
135	114.3	3.1	340	67.22	2700	23.62	516
136	108	4.5	348.1	31.91	3510	32.50	390
137	110	1.9	350	40.50	2200	20.00	368
138	114.3	3.19	414	35.44	838	7.33	756
139	114.3	3.1	340	67.22	2700	23.62	536

Table A1. *Cont.*

S. No	Diameter	Thickness	Yield Strength	Compressive Strength	Length	Length/Diameter	Axial Capacity
140	95	12.7	277	26.22	860	9.05	1008
141	108	4.5	348.1	46.87	3510	32.50	440
142	165	4.7	355	14.44	2477	15.01	800
143	140	5	378.3	37.53	840	6.00	1379
144	108	4.5	259.7	25.48	1994	18.46	495
145	152.4	1.55	330	32.11	1499	9.84	725
146	110	1.9	350	33.40	2200	20.00	368
147	219	4	325	56.60	1000	4.57	1931
148	114	4.44	332	45.00	850	7.46	902
149	108	4.5	348.1	46.87	4158	38.50	298
150	108	4	347.7	40.47	1620	15.00	672
151	152.7	3.15	421	26.89	1676.4	10.98	880.11
152	108	4	338.88	35.71	4320	40.00	294
153	108	4	338.88	35.71	1620	15.00	707.56
154	108	4.2	259.7	25.87	648	6.00	722
155	92	3	260.7	26.07	920	10.00	431
156	108	4	338.88	35.71	864	8.00	869.26
157	219	7	273	46.50	990	4.52	3278
158	108	4.5	344	40.91	548	5.07	917
159	107	4	379.8	38.32	542	5.07	889
160	108	4.5	259.7	25.48	648	6.00	665
161	219	7	273	46.50	990	4.52	3278
162	190.7	6	505	65.44	2300	12.06	2610
163	114	3.31	291	30.00	2320	20.35	535
164	95	12.6	275	25.89	861	9.06	1019
165	114.3	3.1	348	62.67	1020	8.92	845
166	140	5	378.3	42.63	840	6.00	1501
167	88.9	5.842	406	50.50	508	5.71	890
168	95	3.51	340	31.44	1980	20.84	488
169	108	4	338.88	35.71	4320	40.00	345.94
170	127.3	1.63	376	77.20	711	5.59	1285
171	95	3.76	332	31.44	1980	20.84	536
172	165	4.7	355	40.50	2476	15.01	1037
173	166	5	287.14	34.68	3700	22.29	958.44
174	127	2.413	336	27.11	914	7.20	627.2
175	114.3	3.1	340	73.10	3370	29.48	362
176	165	4.7	355	33.40	2475	15.00	1037
177	95	3.66	350	31.11	1981	20.85	529
178	114	1.73	266	40.00	1751	15.36	461
179	219	7	273	46.50	1640	7.49	2956
180	95	3.4	343	30.44	1980	20.84	473
181	210	2.5	237.2	32.93	1670	7.95	1323
182	95	3.78	392	31.44	1980	20.84	567
183	114	5.99	486	45.00	1750	15.35	1177
184	114	3.28	291	43.75	2750	24.12	667
185	108	4	338.88	35.71	5400	50.00	225.4
186	114.3	3.1	340	64.56	3720	32.55	305
187	108	4.5	259.7	25.48	1296	12.00	563
188	165	4.3	317.7	52.30	3640	22.06	987
189	114	3.29	291	30.00	2250	19.74	652
190	166	5	288.1	33.12	1040	6.27	1372
191	114.3	3.1	348	67.22	2040	17.85	617
192	168.3	4.47	302	29.33	813	4.83	1744
193	108	4	327.1	41.55	1188	11.00	686
194	140	5	378.3	51.25	840	6.00	1539
195	101.73	3.1	604.67	37.93	1524	14.98	800.1
196	152.4	1.55	294	43.25	914	6.00	733
197	219	7	273	46.50	1640	7.49	2956
198	168.8	2.64	200.2	42.13	1830	10.84	916
199	108	4	338.88	35.71	648	6.00	828.1
200	165.2	4.1	353	49.88	1322	8.00	1412
201	120.9	5.54	343	30.22	2311	19.11	867
202	114	6.14	486	34.44	2250	19.74	1000
203	166	5	313.6	51.24	1700	10.24	1460.2
204	219	7	273	46.50	1640	7.49	2956
205	76.5	1.73	364	31.11	1524	19.92	245
206	82.55	1.397	482.3	47.29	1117.6	13.54	356
207	95	12.8	283	26.22	1980	20.84	886
208	190.7	6	505	65.44	1150	6.03	3064
209	95	3.4	340	31.44	860	9.05	656

Table A1. *Cont.*

S. No	Diameter	Thickness	Yield Strength	Compressive Strength	Length	Length/Diameter	Axial Capacity
210	114	5.64	486	34.44	2250	19.74	902
211	240	10	269	58.80	1440	6.00	5135
212	152	1.65	270	83.00	900	5.92	1458
213	140	3	426.3	40.38	840	6.00	1208
214	216	6.05	395	29.11	2220	10.28	2462
215	108	4.5	348.1	46.87	4023	37.25	320
216	95	3.58	340	31.44	1420	14.95	576
217	169.3	2.62	338.1	45.13	1830	10.81	756
218	95	12.65	275	25.89	1420	14.95	930
219	114	6.21	486	40.00	2750	24.12	941
220	108	4.5	259.7	25.48	972	9.00	666
221	121	5.56	327	30.67	1050	8.68	1079
222	168.1	4.52	298	52.30	813	4.84	2113
223	216	4.06	289	29.11	2220	10.28	1023
224	114.3	3.1	340	73.10	3370	29.48	401
225	165.2	4.1	353	49.88	2974	18.00	1147
226	140	5.3	378.3	60.56	840	6.00	1664
227	127	2.39	289	42.75	1499	11.80	623

References

1. El-Heweity, M.M. On the performance of circular concrete-filled high strength steel columns under axial loading. *Alex. Eng. J.* **2012**, *51*, 109–119. [CrossRef]
2. Elbakry, H.M.F. A numerical approach for evaluating the stiffness of steel tube–R.C. beam composite joint. *Alex. Eng. J.* **2014**, *53*, 583–589. [CrossRef]
3. Jayalekshmi, S.; Jegadesh, J.S.S.; Goel, A. Empirical approach for determining axial strength of circular concrete filled steel tubular columns. *J. Inst. Eng. Ser. A* **2018**, *99*, 257–268. [CrossRef]
4. Ekmekyapar, T.; AL-Eliwi, B.J.M. Concrete filled double circular steel tube (CFDCST) stub columns. *Eng. Struct.* **2017**, *135*, 68–80. [CrossRef]
5. Chen, D.; Montano, V.; Huo, L.; Fan, S.; Song, G. Detection of subsurface voids in concrete-filled steel tubular (CFST) structure using percussion approach. *Constr. Build. Mater.* **2020**, *262*, 119761. [CrossRef]
6. Chen, D.; Montano, V.; Huo, L.; Song, G. Depth detection of subsurface voids in concrete-filled steel tubular (CFST) structure using percussion and decision tree. *Meas. J. Int. Meas. Confed.* **2020**, *163*, 107869. [CrossRef]
7. Rong, B.; Liu, S.; Li, Z.; Liu, R. Experimental and numerical studies of failure modes and load-carrying capacity of through-diaphragm connections. *Trans. Tianjin Univ.* **2018**, *24*, 387–400. [CrossRef]
8. Alatshan, F.; Osman, S.A.; Mashiri, F.; Hamid, R. Explicit simulation of circular CFST stub columns with external steel confinement under axial compression. *Materials* **2019**, *13*, 23. [CrossRef]
9. Akbar, A.; Farooq, F.; Shafique, M.; Aslam, F.; Alyousef, R.; Alabduljabbar, H. Sugarcane bagasse ash-based engineered geopolymer mortar incorporating propylene fibers. *J. Build. Eng.* **2020**, *33*, 101492. [CrossRef]
10. Ren, Q.; Li, M.; Zhang, M.; Shen, Y.; Si, W. Prediction of ultimate axial capacity of square concrete-filled steel tubular short columns using a hybrid intelligent algorithm. *Appl. Sci.* **2019**, *9*, 2802. [CrossRef]
11. Zhang, T.; Lyu, X.; Yu, Y. Prediction and analysis of the residual capacity of concrete-filled steel tube stub columns under axial compression subjected to combined freeze–thaw cycles and acid rain corrosion. *Materials* **2019**, *12*, 3070. [CrossRef]
12. Ly, H.-B.; Le, T.-T.; Le, L.M.; Tran, V.Q.; Le, V.M.; Vu, H.-L.T.; Nguyen, Q.H.; Pham, B.T. Development of hybrid machine learning models for predicting the critical buckling load of I-shaped cellular beams. *Appl. Sci.* **2019**, *9*, 5458. [CrossRef]
13. Chen, J.B.; Chan, T.M.; Castro, J.M. Parametric study on the flexural behaviour of circular rubberized concrete-filled steel tubes. In *Tubular Structures XVI, Proceedings of the 16th International Symposium on Tubular Structures, ISTS 2017, Melbourne, Australia, 4–6 December 2017*; CRC Press/Balkema: Leiden, The Netherlands, 2018; pp. 51–59.
14. Farooq, F.; Akbar, A.; Khushnood, R.A.; Muhammad, W.L.B.; Rehman, S.K.U.; Javed, M.F. Experimental Investigation of Hybrid Carbon Nanotubes and Graphite Nanoplatelets on Rheology, Shrinkage, Mechanical, and Microstructure of SCCM. *Materials* **2020**, *13*, 230. [CrossRef] [PubMed]
15. Hu, H.S.; Liu, Y.; Zhuo, B.T.; Guo, Z.X.; Shahrooz, B.M. Axial compressive behavior of square CFST columns through direct measurement of load components. *J. Struct. Eng.* **2018**. [CrossRef]

16. Li, G.; Chen, B.; Yang, Z.; Feng, Y. Experimental and numerical behaviour of eccentrically loaded high strength concrete filled high strength square steel tube stub columns. *Thin-Walled Struct.* **2018**, *127*, 483–499. [CrossRef]
17. Mendoza, R.; Yamamoto, Y.; Nakamura, H.; Miura, T. Numerical simulation of compressive failure behaviors of concrete-filled steel tube using coupled discrete model and shell finite element. In *High Tech Concrete: Where Technology and Engineering Meet*; Springer International Publishing: Berlin, Germany, 2018; pp. 1353–1361.
18. Lai, Z.; Varma, A.H. Effective stress-strain relationships for analysis of noncompact and slender filled composite (CFT) members. *Eng. Struct.* **2016**, *124*, 457–472. [CrossRef]
19. Chen, C.C.; Ko, J.W.; Huang, G.L.; Chang, Y.M. Local buckling and concrete confinement of concrete-filled box columns under axial load. *J. Constr. Steel Res.* **2012**, *78*, 8–21. [CrossRef]
20. Mendoza, R.; Yamamoto, Y.; Nakamura, H.; Miura, T. Numerical evaluation of localization and softening behavior of concrete confined by steel tubes. *Struct. Concr.* **2018**, *19*, 1956–1970. [CrossRef]
21. Jumaa, G.B.; Yousif, A.R. Predicting shear capacity of frp-reinforced concrete beams without stirrups by artificial neural networks, gene expression programming, and regression analysis. *Adv. Civ. Eng.* **2018**. [CrossRef]
22. Javed, M.F.; Amin, M.N.; Shah, M.I.; Khan, K.; Iftikhar, B.; Farooq, F.; Aslam, F.; Alyousef, R.; Alabduljabbar, H. Applications of Gene Expression Programming and Regression Techniques for Estimating Compressive Strength of Bagasse Ash based Concrete. *Crystals* **2020**, *10*, 737. [CrossRef]
23. Javed, M.F.; Sulong, N.H.R.; Memon, S.A.; Rehman, S.K.U.; Khan, N.B. FE modelling of the flexural behaviour of square and rectangular steel tubes filled with normal and high strength concrete. *Thin-Walled Struct.* **2017**, *119*, 470–481. [CrossRef]
24. Ferreira, C. Gene Expression Programming: A Newadaptive Algorithm for Solving Problems. Available online: https://scholar.google.com/scholar?hl=en&as_sdt=0%2C5&q=Ferreira%2C+C.%2C+Gene+Expression+Programming%3A+A+New+Adaptive+Algorithm+for+Solving+Problems.+Complex+Systems%2C+2001.+13%282%29%3A+p.+87-129.&btnG= (accessed on 17 December 2019).
25. Sun, Y.; Li, G.; Zhang, J.; Qian, D.; Binh, G.E.; Pham, A. Prediction of the strength of rubberized concrete by an evolved random forest model. *Adv. Civ. Eng.* **2019**. [CrossRef]
26. Zhang, J.; Ma, G.; Huang, Y.; Aslani, F.; Nener, B. Modelling uniaxial compressive strength of lightweight self-compacting concrete using random forest regression. *Constr. Build. Mater.* **2019**. [CrossRef]
27. Kohavi, R. A study of cross-validation and bootstrap for accuracy estimation and model selection. In Proceedings of the International Joint Conference on Artificial Intelligence (IJCAI), Montreal, QC, Canada, 20 August 1995; pp. 1137–1145.
28. Le, L.M.; Ly, H.-B.; Pham, B.T.; Le, V.M.; Pham, T.A.; Nguyen, D.-H.; Tran, X.-T.; Le, T.-T. Hybrid artificial intelligence approaches for predicting buckling damage of steel columns under axial compression. *Materials* **2019**, *12*, 1670. [CrossRef]
29. Sarir, P.; Chen, J.; Asteris, P.G.; Armaghani, D.J.; Tahir, M.M. Developing GEP tree-based, neuro-swarm, and whale optimization models for evaluation of bearing capacity of concrete-filled steel tube columns. *Eng. Comput.* **2019**, *1*, 3. [CrossRef]
30. Elfahham, Y. Estimation and prediction of construction cost index using neural networks, time series, and regression. *Alex. Eng. J.* **2019**, *58*, 499–506. [CrossRef]
31. Diab, A.M.; Elyamany, H.E.; Abd Elmoaty, A.E.M.; Shalan, A.H. Prediction of concrete compressive strength due to long term sulfate attack using neural network. *Alex. Eng. J.* **2014**, *53*, 627–642. [CrossRef]
32. Mohamed, Y.S.; Shehata, H.M.; Abdellatif, M.; Awad, T.H. Steel crack depth estimation based on 2D images using artificial neural networks. *Alex. Eng. J.* **2019**, *58*, 1167–1174. [CrossRef]
33. Mai, S.H.; Seghier, M.E.; Nguyen, P.L.; Jafari-Asl, J.; Thai, D.K. A hybrid model for predicting the axial compression capacity of square concrete-filled steel tubular columns. *Eng. Comput.* **2020**, *1*, 3. [CrossRef]
34. Xu, J.; Wang, Y.; Ren, R.; Wu, Z.; Ozbakkaloglu, T. Performance evaluation of recycled aggregate concrete-filled steel tubes under different loading conditions: Database analysis and modelling. *J. Build. Eng.* **2020**, *30*, 101308. [CrossRef]
35. Zhou, C.; Chen, W.; Ruan, X.; Tang, X. Experimental study on axial compression behavior and bearing capacity analysis of high titanium slag CFST columns. *Appl. Sci.* **2019**, *9*, 2021. [CrossRef]
36. Dao, D.; Trinh, S.; Ly, H.-B.; Pham, B. Prediction of compressive strength of geopolymer concrete using entirely steel slag aggregates: Novel hybrid artificial intelligence approaches. *Appl. Sci.* **2019**, *9*, 1113. [CrossRef]

37. Van Dao, D.; Ly, H.-B.; Vu, H.-L.T.; Le, T.-T.; Pham, B.T. Investigation and optimization of the C-ANN structure in predicting the compressive strength of foamed concrete. *Materials* **2020**, *13*, 1072. [CrossRef] [PubMed]
38. Nguyen, H.Q.; Ly, H.B.; Tran, V.Q.; Nguyen, T.A.; Le, T.T.; Pham, B.T. Optimization of artificial intelligence system by evolutionary algorithm for prediction of axial capacity of rectangular concrete filled steel tubes under compression. *Materials* **2020**, *13*, 1205. [CrossRef]
39. Ly, H.-B.; Pham, B.T.; Le, L.M.; Le, T.-T.; Le, V.M.; Asteris, P.G. Estimation of axial load-carrying capacity of concrete-filled steel tubes using surrogate models. *Neural Comput. Appl.* **2020**. [CrossRef]
40. Nguyen, Q.H.; Ly, H.-B.; Tran, V.Q.; Nguyen, T.-A.; Phan, V.-H.; Le, T.-T.; Pham, B.T. A novel hybrid model based on a feedforward neural network and one step secant algorithm for prediction of load-bearing capacity of rectangular concrete-filled steel tube columns. *Molecules* **2020**, *25*, 3486. [CrossRef]
41. Luat, N.V.; Shin, J.; Lee, K. Hybrid BART-based models optimized by nature-inspired metaheuristics to predict ultimate axial capacity of CCFST columns. *Eng. Comput.* **2020**, *1*, 3. [CrossRef]
42. Han, Q.; Gui, C.; Xu, J.; Lacidogna, G. A generalized method to predict the compressive strength of high-performance concrete by improved random forest algorithm. *Constr. Build. Mater.* **2019**, *226*, 734–742. [CrossRef]
43. Nilsen, V.; Pham, L.T.; Hibbard, M.; Klager, A.; Cramer, S.M.; Morgan, D. Prediction of concrete coefficient of thermal expansion and other properties using machine learning. *Constr. Build. Mater.* **2019**, *220*, 587–595. [CrossRef]
44. Fawagreh, K.; Medhat Gaber, M.; Elyan, E.; Gaber, M.M. Random forests: From early developments to recent advancements. *Syst. Sci. Control Eng. Open Access J.* **2014**, *2*, 602–609. [CrossRef]
45. Ipek, S.; Güneyisi, E.M. Ultimate axial strength of concrete-filled double skin steel tubular column sections. *Adv. Civ. Eng.* **2019**. [CrossRef]
46. Güneyisi, E.M.; Gültekin, A.; Mermerdaş, K. Ultimate capacity prediction of axially loaded CFST short columns. *Int. J. Steel Struct.* **2016**, *16*, 99–114. [CrossRef]
47. Yang, C.; Gao, P.; Wu, X.; Chen, Y.F.; Li, Q.; Li, Z. Practical formula for predicting axial strength of circular-CFST columns considering size effect. *J. Constr. Steel Res.* **2020**, *168*, 105979. [CrossRef]
48. Avci-Karatas, C. Prediction of ultimate load capacity of concrete-filled steel tube columns using multivariate adaptive regression splines (MARS). *Steel Compos. Struct.* **2019**, *33*, 583–594.
49. Wang, X.Y. Optimal design of the cement, fly ash, and slag mixture in ternary blended concrete based on gene expression programming and the genetic algorithm. *Materials* **2019**, *12*, 2448. [CrossRef]
50. Alkroosh, I.S.; Sarker, P.K. Prediction of the compressive strength of fly ash geopolymer concrete using gene expression programming. *Comput. Concr.* **2019**, *24*, 295–302.
51. Iqbal, M.F.; Liu, Q.-F.; Azim, I.; Zhu, X.; Yang, J.; Javed, M.F.; Rauf, M. Prediction of mechanical properties of green concrete incorporating waste foundry sand based on gene expression programming. *J. Hazard. Mater.* **2020**, *384*, 121322. [CrossRef]
52. Bolandi, H.; Banzhaf, W.; Lajnef, N.; Barri, K.; Alavi, A.H. An intelligent model for the prediction of bond strength of FRP bars in concrete: A soft computing approach. *Technologies* **2019**, *7*, 42. [CrossRef]
53. Nour, A.I.; Güneyisi, E.M. Prediction model on compressive strength of recycled aggregate concrete filled steel tube columns. *Compos. Part B Eng.* **2019**, *173*, 106938. [CrossRef]
54. Leon, L.P.; Gay, D. Gene expression programming for evaluation of aggregate angularity effects on permanent deformation of asphalt mixtures. *Constr. Build. Mater.* **2019**, *211*, 470–478. [CrossRef]
55. Gunal, M.; Guven, A.; Asce, M. A genetic programming approach for prediction of local scour downstream hydraulic structures genetic programming approach for prediction of local scour downstream of hydraulic structures. *Artic. J. Irrig. Drain. Eng.* **2008**. [CrossRef]
56. Ferreira, C. *Gene Expression Programming Mathematical Modeling by an Artificial Intelligence*; Springer: Berlin, Germany, 2006; ISBN 3-540-32796-7.
57. Ferreira, C. Gene expression programming in problem solving. In *Soft Computing and Industry*; Springer: London, UK, 2002; pp. 635–653.
58. Tenpe, A.R.; Patel, A. Utilization of support vector models and gene expression programming for soil strength modeling. *Arab. J. Sci. Eng.* **2020**, *45*, 4301–4319. [CrossRef]
59. Nematzadeh, M.; Shahmansouri, A.A.; Fakoor, M. Post-fire compressive strength of recycled PET aggregate concrete reinforced with steel fibers: Optimization and prediction via RSM and GEP. *Constr. Build. Mater.* **2020**, *252*, 119057. [CrossRef]

60. Momeni, M.; Hadianfard, M.A.; Bedon, C.; Baghlani, A. Damage evaluation of H-section steel columns under impulsive blast loads via gene expression programming. *Eng. Struct.* **2020**, *219*, 110909. [CrossRef]
61. Gandomi, A.H.; Roke, D.A. Assessment of artificial neural network and genetic programming as predictive tools. *Adv. Eng. Softw.* **2015**, *88*, 63–72. [CrossRef]
62. Alavi, A.H.; Gandomi, A.H. A robust data mining approach for formulation of geotechnical engineering systems. *Eng. Comput. Int. J. Comput.-Aided Eng.* **2011**, *28*, 242–274.
63. Gandomi, A.H.; Babanajad, S.K.; Alavi, A.H.; Farnam, Y. Novel approach to strength modeling of concrete under triaxial compression. *J. Mater. Civ. Eng.* **2012**. [CrossRef]
64. Muduli, P.K.; Das, S.K.; Bhattacharya, S. CPT-based probabilistic evaluation of seismic soil liquefaction potential using multi-gene genetic programming. *Georisk* **2014**, *8*, 14–28. [CrossRef]
65. Das, S.K. Artificial neural networks in geotechnical engineering: Modeling and application issues. In *Metaheuristics in Water, Geotechnical and Transport Engineering*; Elsevier: Amsterdam, The Netherlands, 2013; pp. 231–270. ISBN 9780123982964.
66. Fulcher, J. Computational intelligence: An introduction. *Stud. Comput. Intell.* **2008**, *115*, 3–78.
67. Alabduljabbar, H.; Haido, J.H.; Alyousef, R.; Yousif, S.T.; McConnell, J.; Wakil, K.; Jermsittiparsert, K. Prediction of the flexural behavior of corroded concrete beams using combined method. *Structures* **2020**, *25*, 1000–1008. [CrossRef]
68. Dunlop, P.; Smith, S. Estimating key characteristics of the concrete delivery and placement process using linear regression analysis. *Civ. Eng. Environ. Syst.* **2003**, *20*, 273–290. [CrossRef]
69. Han, L.H.; Li, W.; Bjorhovde, R. Developments and advanced applications of concrete-filled steel tubular (CFST) structures: Members. *J. Constr. Steel Res.* **2014**, *100*, 211–228. [CrossRef]
70. Ferreira, C. Function finding and the creation of numerical constants in gene expression programming. In *Advances in Soft Computing*; Springer: London, UK, 2003; pp. 257–265.
71. Babanajad, S.K.; Gandomi, A.H.; Alavi, A.H. New prediction models for concrete ultimate strength under true-triaxial stress states: An evolutionary approach. *Adv. Eng. Softw.* **2017**, *110*, 55–68. [CrossRef]
72. Soleimani, S.; Rajaei, S.; Jiao, P.; Sabz, A.; Soheilinia, S. New prediction models for unconfined compressive strength of geopolymer stabilized soil using multi-gen genetic programming. *Meas. J. Int. Meas. Confed.* **2018**, *113*, 99–107. [CrossRef]
73. Kupper, L.L. Probability, statistics, and decision for civil engineers. *Technometrics* **1971**, *13*, 211. [CrossRef]
74. Frank, I.; Todeschini, R. The data analysis handbook. *Data Handl. Sci. Technol.* **1994**, *14*, 1–352.
75. Golbraikh, A.; Tropsha, A. Beware of q2! *J. Mol. Graph. Model.* **2002**. [CrossRef]
76. Gandomi, A.H.; Alavi, A.H.; Mirzahosseini, M.R.; Nejad, F.M. Nonlinear genetic-based models for prediction of flow number of asphalt mixtures. *J. Mater. Civ. Eng.* **2011**, *23*, 248–263. [CrossRef]
77. Roy, P.P.; Roy, K. On some aspects of variable selection for partial least squares regression models. *QSAR Comb. Sci.* **2008**, *27*, 302–313. [CrossRef]
78. Lu, Z.; Zhao, Y. Suggested empirical models for the axial capacity of circular CFT stub columns. *J. Constr. Steel Res.* **2010**. [CrossRef]
79. Goode, C.; Narayanan, R. Design of concrete filled steel tubes to EC4. In Proceedings of the ASCCS Seminar on Concrete Filled Steel Tubes—A Comparison of International Codes and Practice, Innsbruck, Austria, 18 September 1997; pp. 1–25.
80. Giakoumelis, G.; Lam, D. Axial capacity of circular concrete-filled tube columns. *J. Constr. Steel Res.* **2004**, *60*, 1049–1068. [CrossRef]